

KfK 3201  
Oktober 1981

# **Optical Constants of Liquid UO<sub>2</sub> in the Visible Spectral Range Obtained from Reflectivity Measurements**

**M. Bober, J. Singer, K. Wagner  
Institut für Neutronenphysik und Reaktortechnik  
Projekt Schneller Brüter**

**Kernforschungszentrum Karlsruhe**



KERNFORSCHUNGSZENTRUM KARLSRUHE  
Institut für Neutronenphysik und Reaktortechnik  
Projekt Schneller Brüter

KfK 3201

Optical Constants of Liquid  $\text{UO}_2$  in the Visible Spectral  
Range Obtained from Reflectivity Measurements

M. Bober, J. Singer, K. Wagner

The topic of this report was presented at the 8th Symposium  
on Thermophysical Properties, June 15-18, 1981, National  
Bureau of Standards, Gaithersburg, Md., USA.

Kernforschungszentrum Karlsruhe GmbH, Karlsruhe

Als Manuskript vervielfältigt  
Für diesen Bericht behalten wir uns alle Rechte vor

Kernforschungszentrum Karlsruhe GmbH  
ISSN 0303-4003

## Abstract

The optical constants,  $n, k$ , of liquid urania were determined from reflectivity measurements with plane-polarized light. Measurements were made with an integrating-sphere laser reflectometer in the wavelength range 450-750 nm at temperatures between 3000 and 4000 K. Consistent results have been obtained for different angles of incidence. The optical constants show little variation with the wavelength and temperature. Liquid urania proves to be opaque to radiation in the whole spectral range studied. Average values of  $n=1.7$  and  $k=0.8$  are given for the temperature range 3100-3600 K. From this result it is concluded that internal thermal radiation cannot cause a significant increase in thermal conductivity of urania upon melting.

Bestimmung der optischen Konstanten von flüssigem  $UO_2$  im sichtbaren Spektralbereich aus Reflexionsmessungen

---

## Zusammenfassung

Die optischen Konstanten,  $n, k$ , von flüssigem  $UO_2$  wurden aus Reflexionsmessungen mit linear-polarisiertem Licht bestimmt. Die Messungen wurden mit einem integrierenden Laser-Kugelreflektometer in dem Wellenlängenbereich 450-750 nm bei Temperaturen zwischen 3000 und 4000 K durchgeführt. Für verschiedene Reflexionswinkel ergaben sich konsistente Resultate. Die optischen Konstanten zeigen nur eine geringe Abhängigkeit von der Wellenlänge und von der Temperatur. Flüssiges  $UO_2$  erweist sich als opak in dem gesamten untersuchten Spektralbereich. Für den Temperaturbereich 3100-3600 K werden Mittelwerte von  $n=1.7$  und  $k=0.8$  angegeben. Aus diesem Ergebnis wird geschlossen, daß innere thermische Strahlung keinen wesentlichen Anstieg der Wärmeleitfähigkeit von  $UO_2$  beim Schmelzen verursachen kann.

## 1. Introduction

The safety analysis of fast breeder reactors requires information on the thermal radiation properties of the oxide fuel material at temperatures well in excess of its melting point. These radiation properties are characterized by the optical constants of the fuel, i.e. the refractive index,  $n$ , and the absorption constant,  $k$ . Knowledge of the optical constants allows to estimate the magnitude of the internal radiative heat transfer and of the radiative heat losses at the fuel boundary. It could also help in the determination of the physical structure of the liquid fuel.

According to thermal diffusivity measurements on liquid  $\text{UO}_2$  [1], a significant increase in the thermal conductivity of the oxide fuel is observed upon melting. This increase may originate in an augmentation of the radiative [2,3] and the electronic [4,5] heat transport. To estimate the magnitude of the radiative contribution, the wavelength-dependence of the absorption coefficient must be evaluated from the infrared to the visible wavelengths. Previous evaluations were based on the lower-temperature absorption data of single-crystal  $\text{UO}_2$  extrapolated into the liquid state [2,5]. The only experimental data available were the low-temperature values of the refractive index determined in the visible range [6], and of the spectral absorption coefficient measured from the near-infrared to the absorption edge in the visible red [5,7,8]. High-temperature spectral absorption data are urgently needed so that the radiative heat transfer in molten  $\text{UO}_2$  can be reliably calculated. Preliminary values of the optical constants for liquid  $\text{UO}_2$ ,  $n=2$  and  $k=0.6$ , obtained at three wavelengths in the visible range, have been published recently [9,10].

The optical constants of liquid  $\text{UO}_2$  result from high-temperature reflectance measurements performed with plane-polarized light. Such reflectance measurements have been made again at various wavelengths in the visible spectral range between 450 and 750 nm. From the reflectivity measured versus the angle of incidence the optical constants of liquid  $\text{UO}_2$  are inferred by application of the generalized Fresnel reflection equations.

## 2. Measurement technique

Spectral reflectance measurements of liquid  $\text{UO}_2$  have been carried out with an integrating-sphere laser reflectometer which operates with laser-beam heating. The experimental setup has been described in detail elsewhere [11,12].

Fig.1 shows schematically the principle of the measurement apparatus. A small specimen of  $\text{UO}_2$  is located in an integrating sphere of 200 mm diameter. With a focussed  $\text{CO}_2$ -laser beam of 500W power the surface of the specimen is locally heated for millisecond intervals to temperatures between 3000 and 4000 K. The quasi-isothermally heated surface area is about 0.5 mm in diameter. The maximum temperature and the heating rate can be varied by variation of the laser power density. The center of the heated surface area is simultaneously irradiated by the light beam of a reference laser set at the measurement wavelength. The reflected portion of the reference light is isotropically scattered by the diffuse-reflective integrating sphere and measured with a spectral photomultiplier detector placed at a small aperture in the sphere well.

A spectral line filter of the measurement wavelength placed in front of the detector, together with modulation of the incident reference light at 200 kHz, permits the selective detection of the reflected light in the presence of the thermal radiation background emitted from the heated sample. The

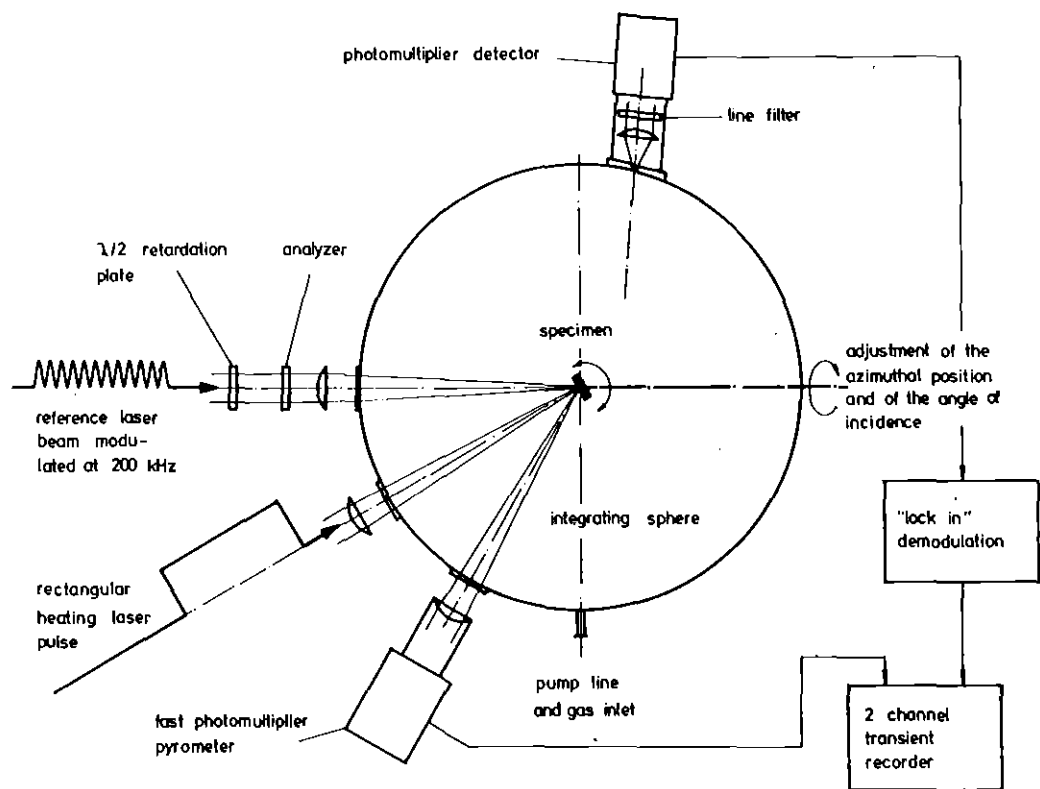


Fig.1: Principle of measurement technique.

demodulated reflection signal then yields the reflectance of the sample by means of an additional calibration measurement where the  $\text{UO}_2$  specimen is replaced by a reflectance standard made of freshly pressed Halon<sup>1)</sup> [13].

During the reflection measurements a pure inert gas atmosphere is maintained in the sphere at 2 bar pressure level to suppress surface evaporation of the sample. The surface temperature of the heated sample is determined by means of a fast micropyrometer working at the wavelength 633 nm, at which the spectral emittance of liquid  $\text{UO}_2$  is known [14]. The angle of incidence of the reference light can be set between 5 and  $75^\circ$  with an accuracy of  $\pm 0.3^\circ$  by altering the inclination of the sample. By use of a half-wave retarder together with an analyzer, the plane of polarization of the incident light is precisely adjusted with respect to the plane of incidence. Reference light sources are krypton-ion and argon-ion lasers of some 100 mW rms power when modulated; they allow measurements at about 10 wavelengths in the visible range 400–750 nm. For future experiments a high-power Nd:YAG laser will be available for heating which will produce larger heated surface areas and higher temperatures and permit additional reflectance measurements to be made at the laser wavelength of 1064 nm.

### 3. Evaluation method

Reflectance measurements performed with plane-polarized monochromatic radiation at non-normal incidence allow the optical constants of the sample material to be determined, provided that the specimen surface is optically smooth. The optical constants,  $n$  and  $k$ , are both functions of the temperature,  $T$ , and wavelength,  $\lambda$ . The absorption constant,  $k$ , is related to the absorption coefficient,  $\alpha_{\lambda,T}$ , as measured by the transmission method, by the equation:

---

1) A powdered fluorocarbon manufactured by Allied Chemical Corporation, NJ.

$$\alpha_{\lambda,T} = 4\pi k/\lambda. \quad (1)$$

The reciprocal of  $\alpha_{\lambda,T}$  is the mean free path of the radiation in the material. This is the characteristic quantity which, in a spectrally averaged form, enters the expression for the radiative heat transfer given in the Rosseland diffusion approximation [15].

The optical constants can be evaluated from reflectance measurements by analyzing the variation of the reflected energy with the angle of incidence and the state of polarization of the incident light. Suitable parameters to measure are the reflectances  $\rho_{\parallel}$  and  $\rho_{\perp}$  for the incident radiation polarized parallel and perpendicular, respectively, to the plane of incidence, the intensity ratio of  $\rho_{\parallel}$  and  $\rho_{\perp}$ , and the relative phase difference [16]. One evaluation method is based solely on the measurement of the intensity ratio of  $\rho_{\parallel}$  and  $\rho_{\perp}$  at two different angles of incidence [17]. This method has been shown to be appropriate for the reflectivity measurements performed on molten UO<sub>2</sub> in an integrating-sphere reflectometer [9,10].

Mathematical expressions based on the generalized Fresnel reflection equations can be obtained for the parallel and perpendicular reflectivity components, which are related to the optical constants and to the angle of incidence,  $\theta$ , as follows [18]:

$$\rho_{\perp}(\theta) = \frac{(a-\cos\theta)^2 + b^2}{(a+\cos\theta)^2 + b^2} \quad (2)$$

$$\rho_{\parallel}(\theta) = \rho_{\perp}(\theta) \frac{(a-\sin\theta\tan\theta)^2 + b^2}{(a+\sin\theta\tan\theta)^2 + b^2} \quad (3)$$

where

$$a^2 = \frac{1}{2} \{ (n^2 - k^2 - \sin^2 \theta) + [(n^2 - k^2 - \sin^2 \theta)^2 + 4n^2 k^2]^{1/2} \}$$

$$b^2 = \frac{1}{2} \{ -(n^2 - k^2 - \sin^2 \theta) + [(n^2 - k^2 - \sin^2 \theta)^2 + 4n^2 k^2]^{1/2} \}.$$

These relations are used for the evaluation of the reflectance measurements. The accuracy of the evaluation is improved by using the ratio  $\rho_{\parallel}/\rho_{\perp}$ , as this ratio varies more rapidly with the angle of incidence than  $\rho_{\parallel}$  and  $\rho_{\perp}$  alone, and because, in principle, absolute reflectance measurements are not necessary. This is illustrated by Fig.2 which shows the reflectivity components as a function of  $\theta$ , calculated from the equations (2) and (3) with the preliminary values of  $n, k$  for liquid  $UO_2$  [9,10]. The angle,  $\theta_o$ , near the angle where  $\rho_{\parallel}/\rho_{\perp}$  is minimum, is the principal angle of incidence at which  $\rho_{\parallel}$  and  $\rho_{\perp}$  differ in phase by  $90^\circ$ .  $\theta_o$  is related to  $n$  and  $k$  by [19]:

$$(n^2 + k^2)^2 - 2(n^2 - k^2)\sin^2 \theta_o = (\tan^4 \theta_o - 1)\sin^4 \theta_o. \quad (4)$$

The evaluation method requires a suitable choice of the measurement angles,  $\theta$ , [20]. The highest sensitivity, for  $n$  and  $k$  is reached if the angles of incidence are chosen such that one is just below, and the other just above, the principal angle of incidence. This appears from the isoreflectance curves of  $\rho_{\parallel}/\rho_{\perp}$  in the  $n-k$  plane, as shown in Fig.3 for the case of  $n=2.0$  and  $k=0.6$ . Each curve represents a set of  $n, k$  values which fulfil equation (3) for one distinct angle  $\theta$  in the ranges of  $1.7 \leq n \leq 2.3$  and  $0.3 \leq k \leq 0.9$ . The maximum accuracy in evaluation is obtained if the chosen angles of incidence correspond with isoreflectance curves which intersect nearly perpendicularly. In order to get reliable values of  $n$  and  $k$  the measurements should include a third intermediate angle near the principal angle of incidence. With this third angle the measurements can be averaged for  $n$  and  $k$  and the consistence of the three values of  $n$  and  $k$  obtained can serve as a control of the accuracy of the measurements.

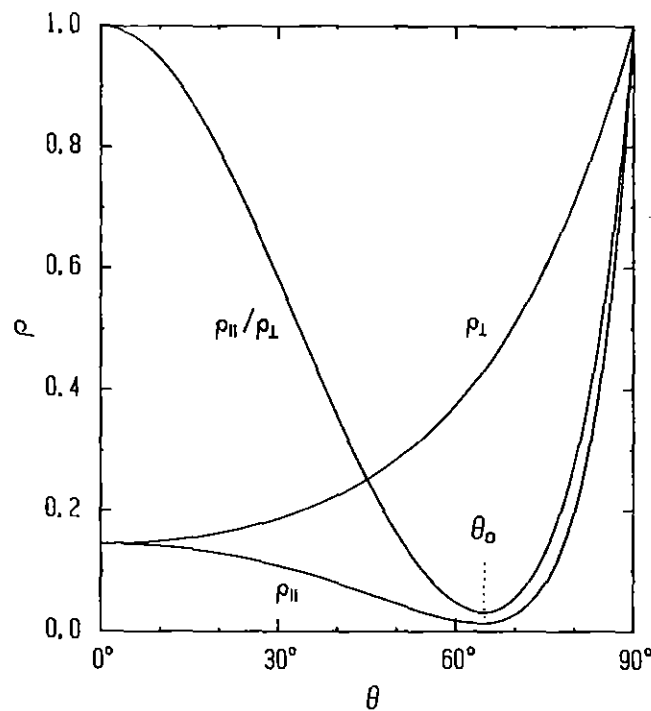


Fig.2: Calculated reflectivity curves for  $n=2$ ,  $k=0.6$ . (equations (2) and (3)).

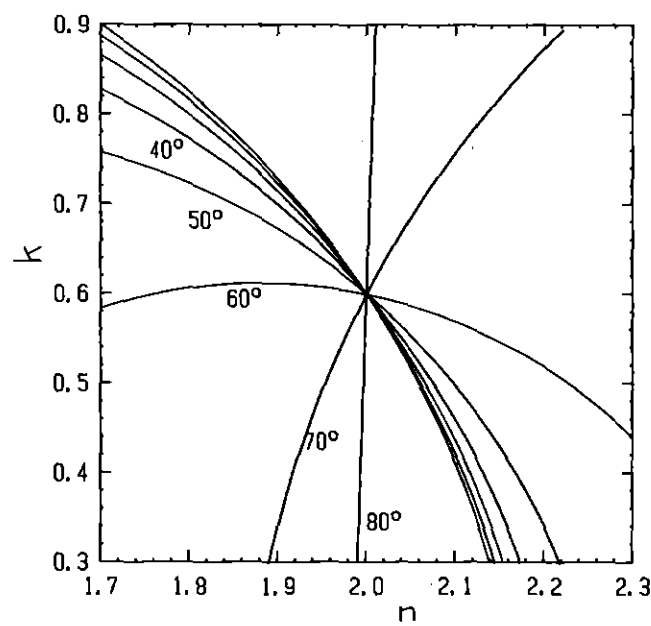


Fig.3: Isoreflectance curves of  $\rho_{\parallel} / \rho_{\perp}$  in the  $n-k$  plane calculated for  $n=2$ ,  $k=0.6$  at different angles of incidence. (equation (3)).

A useful relation between  $\rho_{\parallel}$  and  $\rho_{\perp}$  follows from equation (3) for the case of  $\theta=45^{\circ}$ :

$$\rho_{\parallel} = \rho_{\perp}^2. \quad (5)$$

This allows to check the accuracy of the reflectivity of the two components measured at this angle.

#### 4. Measurements and results

The reflectance of liquid  $\text{UO}_2$  has been measured with polarized light in the temperature range 3000–4000K at the four wavelengths 458, 514.5, 647 and 752.5 nm, and at angles of incidence 45, 58 and  $71^{\circ}$ . Suitable angles have been chosen according to the isoreflectance curves shown in Fig.3. The specimen material used was nuclear-reactor grade, stoichiometric  $\text{UO}_2$  sintered to 96% of the theoretical density with residual impurities of <100 ppm C and 200 ppm Si+Cr+Fe. Smooth surfaced samples have been generated by degassing and liquefying the surface layer of plane specimen disks (6mm in diameter and 1mm thick), applying surface heating with the  $\text{CO}_2$ -laser beam immediately before measurements. Figs.4 and 5 show the molten surface zone of a  $\text{UO}_2$  specimen,  $\approx 1$  mm in diameter, and the SEM micrograph of a rupture across the refrozen surface.

To improve the generation of the liquid layer on the specimen surface a double pulse heating technique has been applied. The first pulse serves to prepare the surface, the second pulse yields the actual measurement signal for evaluation. Fig.6 shows a typical record obtained with the digital oscilloscope for a  $\text{UO}_2$  sample. The upper trace represents the reflectivity signal  $\rho_{\perp}$ , the lower trace is the pyrometer signal. The fixed-point plateau at the end of the pyrometer signal indicates the freezing point. The reflectivity signal reveals a decrease of the reflectance with increasing temperature.

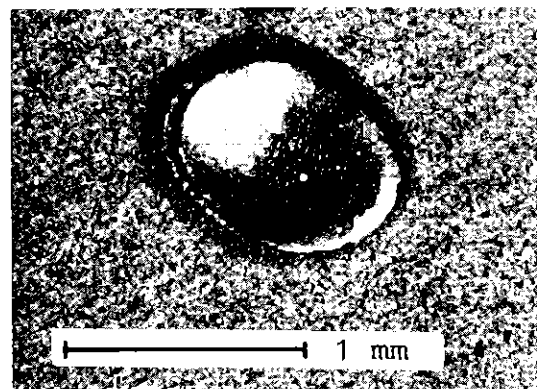


Fig.4: Refrozen molten surface zone of a  $\text{UO}_2$  specimen.

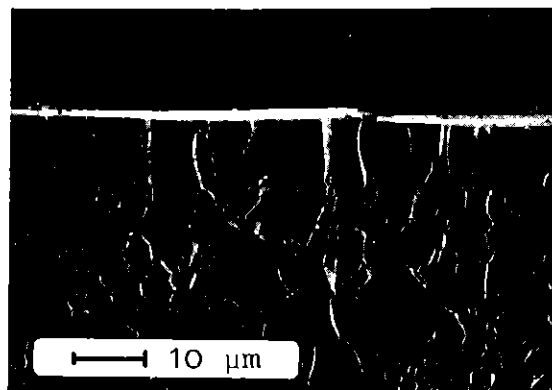


Fig.5: SEM micrograph of a rupture across the refrozen molten layer, 10  $\mu\text{m}$  thick, on the surface of  $\text{UO}_2$ .

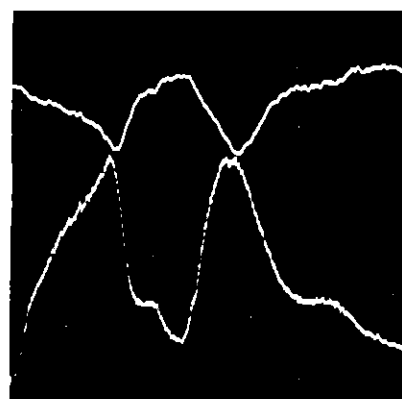


Fig.6: Digital oscilloscope recordings of reflectivity,  $\rho_\perp$ , (upper trace) and pyrometer signal (lower trace), respectively, obtained with  $\text{UO}_2$  at  $\lambda=647 \text{ nm}$  and  $\theta=58^\circ$ .  $T_{\max} \approx 3630 \text{ K}$  Sweptime=6 ms.

Between 20 and 25 series of measurements have been evaluated for each wavelength and each angle of incidence. The resulting reflectivities obtained for the parallel and perpendicular components,  $\rho_{\parallel}$  and  $\rho_{\perp}$ , are shown in Fig. 7 as a function of the temperature. The scatter of the individual data points, which are plotted together with the average curves of  $\rho_{\parallel}$  and  $\rho_{\perp}$ , indicates the range of uncertainty of the single measurements. Fig. 7 shows that liquid  $\text{UO}_2$  behaves similarly in the whole visible spectral range. There is little variation of the measured reflectivity with the wavelength, and all reflectivity curves show a similar dependence on the temperature. Only the variation of the reflectivity with the angle of incidence is evident. In accordance with the Fresnel reflection equations, the reflectivity for the component  $\rho_{\perp}$  clearly increases with increasing angle of incidence whereas  $\rho_{\parallel}$  passes through a minimum (cf. Fig. 2).

Table I gives values of the spectral reflectivity of liquid  $\text{UO}_2$  averaged at different temperatures for the three measurement angles of the polarized components  $\rho_{\parallel}$  and  $\rho_{\perp}$ . It can be seen that equation (5) is well fulfilled for  $\theta=45^\circ$ . The ratios  $\rho_{\parallel}/\rho_{\perp}$  listed in Table I have been used to evaluate the optical constants of  $\text{UO}_2$ . For each pair of measurement angles these values have been introduced in equation (3) and the corresponding values of  $n$  and  $k$  have been computed which satisfy simultaneously the equation for both  $\rho_{\parallel}/\rho_{\perp}$  ratios. Results for the temperature range 3100–3600K are given in Tables II and III.

Table II shows the values of the optical constants obtained from the three pairs of measurement angles; Table III gives the average values. Obviously, the optical constants of liquid  $\text{UO}_2$  vary only slightly with the wavelength and temperature. The absorption constant is relatively high, indicating strong absorption in the visible spectral range with a slight increase perceptible at both ends of the spectrum. Both values,  $n$  and  $k$ , show a tendency to decrease with increasing temperature. The plot of  $n$  and  $k$  versus the wavelength is given in Fig. 8 where the data points are connected by straight lines.

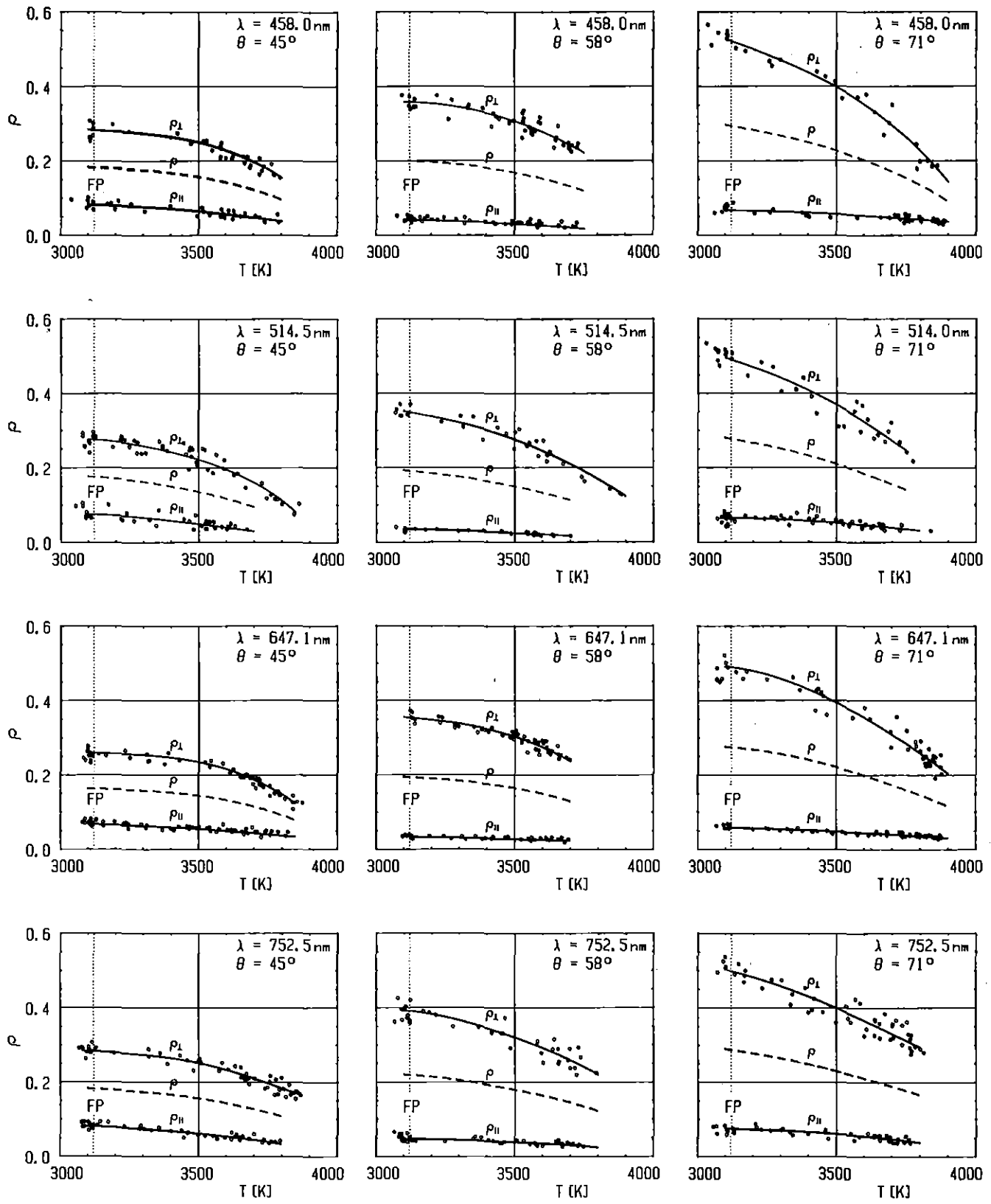


Fig.7: Spectral reflectivity of liquid  $\text{UO}_2$  at various wavelengths in the visible range measured at three angles of incidence as a function of the temperature.  $\rho_{\parallel}$  and  $\rho_{\perp}$  are the parallel and perpendicular components, respectively, and  $\rho$  is that of unpolarized radiation ( $\rho = 0.5(\rho_{\parallel} + \rho_{\perp})$ ). FP=frosting point.

Table I Values of the spectral reflectivity of liquid  $\text{UO}_2$  averaged at different temperatures for three angles of incidence of the polarized components  $\rho_{\parallel}$  and  $\rho_{\perp}$ .

$\lambda$ (nm)	T (K)	$\theta = 45^\circ$			$\theta = 58^\circ$			$\theta = 71^\circ$		
		$\rho_{\parallel}$	$\rho_{\perp}$	$\rho_{\parallel}/\rho_{\perp}$	$\rho_{\parallel}$	$\rho_{\perp}$	$\rho_{\parallel}/\rho_{\perp}$	$\rho_{\parallel}$	$\rho_{\perp}$	$\rho_{\parallel}/\rho_{\perp}$
458	3100	0.080	0.282	0.283	0.041	0.358	0.115	0.065	0.525	0.124
458	3200	0.078	0.278	0.280	0.040	0.352	0.113	0.064	0.501	0.128
458	3300	0.074	0.272	0.274	0.037	0.343	0.108	0.063	0.470	0.133
458	3400	0.069	0.262	0.264	0.034	0.328	0.103	0.060	0.437	0.137
458	3500	0.062	0.248	0.250	0.031	0.307	0.100	0.056	0.399	0.140
458	3600	0.052	0.227	0.230	0.027	0.280	0.095	0.052	0.353	0.147
514.5	3100	0.075	0.277	0.271	0.034	0.350	0.096	0.065	0.498	0.130
514.5	3200	0.071	0.270	0.262	0.032	0.336	0.096	0.064	0.473	0.135
514.5	3300	0.065	0.260	0.252	0.030	0.320	0.094	0.061	0.443	0.139
514.5	3400	0.058	0.245	0.238	0.027	0.300	0.090	0.058	0.406	0.142
514.5	3500	0.049	0.224	0.220	0.024	0.275	0.088	0.052	0.367	0.143
514.5	3600	0.039	0.195	0.199	0.020	0.245	0.080	0.046	0.323	0.141
647	3100	0.069	0.263	0.262	0.033	0.355	0.094	0.058	0.491	0.118
647	3200	0.067	0.260	0.259	0.032	0.348	0.093	0.056	0.479	0.117
647	3300	0.066	0.256	0.257	0.031	0.338	0.093	0.054	0.461	0.117
647	3400	0.063	0.250	0.251	0.030	0.324	0.092	0.052	0.431	0.120
647	3500	0.056	0.236	0.237	0.028	0.305	0.092	0.048	0.394	0.122
647	3600	0.046	0.214	0.214	0.025	0.276	0.091	0.044	0.353	0.124
752.5	3100	0.081	0.285	0.284	0.047	0.393	0.119	0.075	0.501	0.149
752.5	3200	0.078	0.279	0.279	0.046	0.384	0.120	0.073	0.479	0.151
752.5	3300	0.073	0.271	0.270	0.044	0.367	0.120	0.070	0.455	0.153
752.5	3400	0.069	0.262	0.261	0.042	0.346	0.122	0.066	0.428	0.155
752.5	3500	0.062	0.250	0.249	0.039	0.321	0.122	0.061	0.397	0.155
752.5	3600	0.054	0.232	0.235	0.035	0.293	0.121	0.055	0.365	0.151

Table II Values of the optical constants of liquid UO<sub>2</sub>, calculated for each pair of measurement angles with the  $\rho_{\parallel}/\rho_{\perp}$  ratios of Table I.  
(equation (3)).

$\lambda$ (nm)	T (K)	$\theta_1=45^\circ, \theta_2=58^\circ$		$\theta_1=45^\circ, \theta_2=71^\circ$		$\theta_1=58^\circ, \theta_2=71^\circ$	
		n	k	n	k	n	k
458	3100	1.72	0.94	1.78	0.92	1.80	0.95
458	3200	1.71	0.92	1.76	0.91	1.77	0.93
458	3300	1.71	0.90	1.73	0.89	1.74	0.90
458	3400	1.67	0.86	1.70	0.86	1.71	0.87
458	3500	1.61	0.83	1.67	0.81	1.68	0.85
458	3600	1.53	0.77	1.63	0.75	1.65	0.81
514.5	3100	1.74	0.84	1.72	0.85	1.72	0.84
514.5	3200	1.67	0.83	1.69	0.82	1.70	0.84
514.5	3300	1.62	0.80	1.67	0.79	1.67	0.82
514.5	3400	1.57	0.76	1.64	0.74	1.65	0.79
514.5	3500	1.50	0.72	1.62	0.68	1.64	0.78
514.5	3600	1.46	0.65	1.61	0.59	1.64	0.74
647	3100	1.76	0.84	1.78	0.83	1.78	0.84
647	3200	1.75	0.83	1.78	0.82	1.78	0.83
647	3300	1.74	0.82	1.78	0.81	1.78	0.83
647	3400	1.70	0.81	1.76	0.79	1.77	0.82
647	3500	1.61	0.78	1.73	0.74	1.75	0.82
647	3600	1.50	0.73	1.69	0.65	1.74	0.82
752.5	3100	1.70	0.95	1.68	0.96	1.67	0.94
752.5	3200	1.65	0.94	1.66	0.94	1.66	0.94
752.5	3300	1.60	0.92	1.64	0.91	1.65	0.94
752.5	3400	1.52	0.89	1.63	0.88	1.65	0.95
752.5	3500	1.45	0.85	1.62	0.83	1.65	0.95
752.5	3600	1.40	0.81	1.62	0.77	1.67	0.95

Table III Optical constants of solid and liquid  $\text{UO}_2$  at different temperatures, averaged for the wavelengths 458, 514.5, 647 and 752.5 nm.

T (K)	458 nm		514.5 nm		647 nm		752.5 nm	
	n	k	n	k	n	k	n	k
300	2.21	0.84	2.25	0.76	2.24	0.77	2.25	0.60
3100	1.77	0.94	1.73	0.84	1.77	0.84	1.68	0.95
3200	1.75	0.92	1.69	0.83	1.77	0.83	1.66	0.94
3300	1.73	0.90	1.65	0.80	1.77	0.82	1.63	0.92
3400	1.69	0.86	1.62	0.76	1.74	0.81	1.60	0.91
3500	1.65	0.83	1.59	0.73	1.70	0.78	1.57	0.88
3600	1.60	0.78	1.57	0.66	1.64	0.73	1.56	0.84

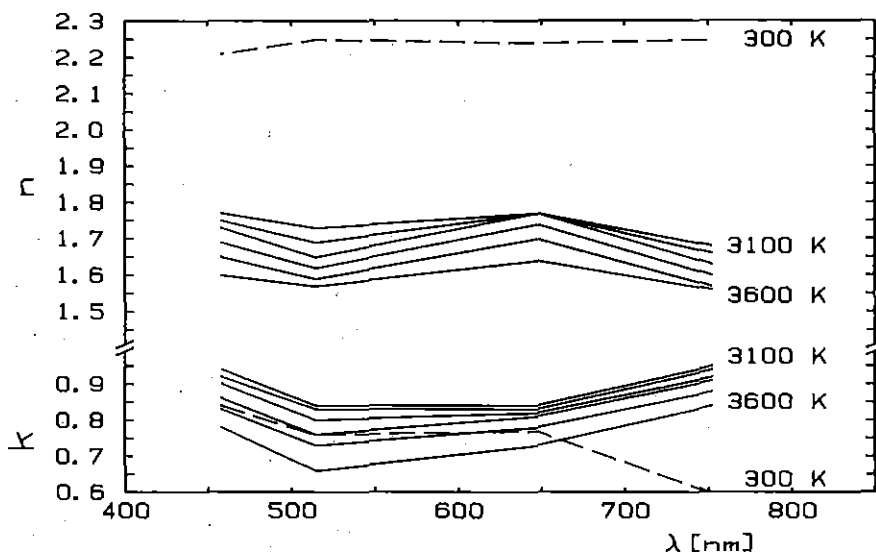


Fig.8: Optical constants of solid (broken line) and liquid  $\text{UO}_2$  as a function of the wavelength .

For comparison Table III and Fig.8 additionally show values of n and k obtained from reflectivity measurements with single crystal  $\text{UO}_2$  at room temperature. The n values and the spectral course (broken line) are in good agreement with the result of Ackermann et al. /6/. Contrary to the k values of liquid  $\text{UO}_2$  the room temperature values of k decrease at the red end of the spectrum as shown in the diagram of Fig.8.

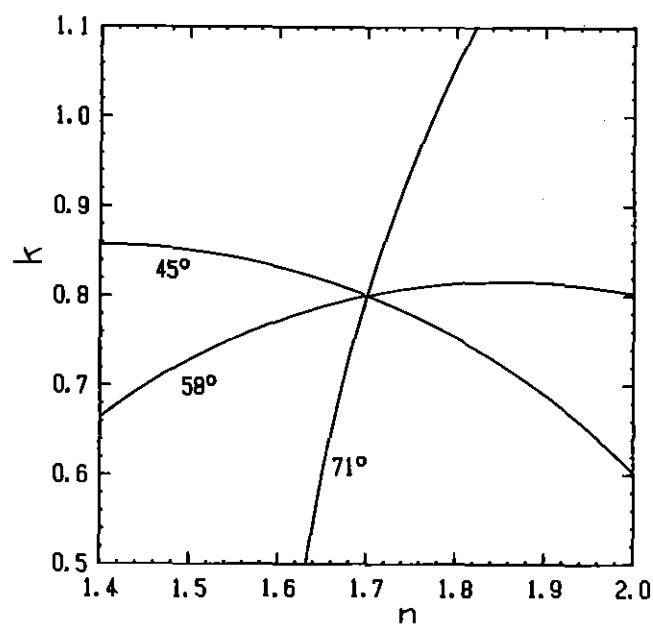
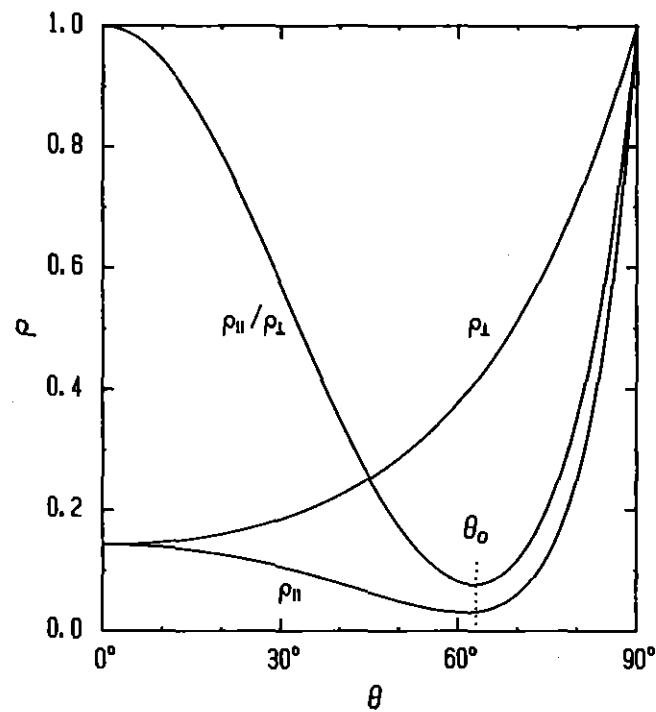


Fig.9: Calculated reflectivity curves for  $n=1.7$  and  $k=0.8$  (equations (2) and (3)), and the corresponding isoreflectance curves of  $\rho_{\parallel}/\rho_{\perp}$  obtained in the  $n-k$  plane for the measurement angles.

Considering this diagram, average values of  $n=1.7$  and  $k=0.8$  can be proposed to be representative for the visible spectrum and the temperature range 3100–3600 K. Fig. 9 show the reflectivity curves calculated for  $n=1.7$  and  $k=0.8$ , and the corresponding reflectance curves of  $\rho_{\parallel}/\rho_{\perp}$  obtained for the measurement angles 45, 58 and 71°. On account of the scatter in the reflectance data (Fig. 7), the uncertainty in the values of  $n$  and  $k$  (given in Table III) can be estimated to be  $\pm 10\%$  and  $\pm 20\%$ , respectively. A simple control of the accuracy is obtained from the consideration of the consistency of the three values of  $n$  and  $k$  derived from the three pairs of measurement angles. As shown in Table II, the respective values agree very well. Up to temperatures of 3500 K the deviations from the average are even less than 8 %, but with increasing temperature the agreement diminishes.

### 5. Discussion

The Fresnel formulas used to calculate the optical constants from the measured reflectivity ratios are based on the assumption of an ideal optically smooth surface, a condition which is difficult to attain. The scatter in the experimental values shown in Fig. 7 can be mainly attributed to the imperfections of the reflecting surface and to variations in the true angle of incidence caused by oscillations of the liquid surface layer and the formation of a meniscus. With increasing temperature, vaporization and gas bursts disturb the smoothness of the surface which then gives a certain amount of diffuse reflection. The effect of this is apparent from the decreasing consistency of the results for temperatures above 3500 K which have been obtained from measurements at different angles of incidence. It can be inferred also from the check of the measurements at 45° incidence made with equation (5), which proves to be less satisfied at the higher temperatures than at the lower ones. Therefore, the evaluation of the optical constants has been limited to temperatures up to 3600 K.

The sensitivity of  $n$  and  $k$  to the errors of the reflectivity measurements depends on the magnitude of  $n$  and  $k$  [20]. For the case of  $UO_2$ , the accuracy of  $k$  is more influenced by measurement errors than that of  $n$ . This is also apparent from

the uncertainty in the values of  $n$  and  $k$  produced by the scatter in the measurement points. Besides, the average margin of the scatter corresponds to a variation in the true angles of incidence of  $\pm 3^\circ$  if other measurement errors are disregarded.

An estimate of the systematic errors which may be involved is particularly difficult. For example, chemical impurities in the surface layer or errors in the adjustment of the apparatus can bias the resulting values of  $n$  and  $k$ . So, a misadjustment of the angle of incidence could be responsible for the deviation of the preliminary values,  $n=2$  and  $K=0,6$  [9,10], from the actual values. For the actual measurements described here, the adjustments of the apparatus were improved so that large errors are unlikely to occur. This is shown evidently by the good mutual agreement of the three values of  $n$  and  $k$  obtained from the different pairs of measurement angles. The specimen material used was nuclear-reactor grade fuel material. An influence of the residual chemical impurities of the sample material on the resulting optical constants cannot be excluded. However, because of the preheating and outgassing of the liquid surface layer prior to the measurements, the influence of the impurities should have been reduced.

The tendency of  $n$  and  $k$  to decrease with increasing temperature is plausible to some degree because the variation goes in the direction of decreasing density of the liquid. The value of the average refractive index,  $n=1.7$ , found for molten  $UO_2$  is smaller than that of 2.3 reported by Ackermann et al. [6] at room temperature. This decrease in  $n$  may be explained by assuming a decrease in the electronic polarizability of  $UO_2$  upon melting [3]. The plot of the absorption constant  $k$  of liquid  $UO_2$  depicted in Fig. 8 shows no decrease at the red end of the spectrum. Obviously, the position of the fundamental absorption edge of  $UO_2$  is shifted from its room temperature value of 600 nm to longer wavelengths. A corresponding shift of the edge to 900 nm was observed by Davies [8] at the temperature of 1200 K. That means, liquid  $UO_2$  is opaque in the visible and near infrared spectral range, and there appears no trans-

parency upon melting as it was assumed [3]. This is in accordance with the theoretical arguments of MacInnes [4] predicting an increase in the electronic activity of  $\text{UO}_2$  at high temperatures about the melting point which should greatly decrease the optical transmission.

According to the thermal diffusivity measurements of Kim et al. [1], an increase in the thermal conductivity of  $\text{UO}_2$  is expected upon melting from 0.04 to ca. 0.1 W/cmK. Extrapolating the room-temperature absorption data of  $\text{UO}_2$  Browning [5] concluded that only 10 % of this value can be explained by the radiative contribution if an absorption coefficient  $\alpha \geq 10^3 \text{ cm}^{-1}$  is true for the visible spectral range. This conclusion has been proven by the present investigation. The average value  $k = 0.8$  corresponds to an absorption coefficient,  $\alpha \approx 10^5 \text{ cm}^{-1}$  (equation (1)), i.e. to a mean free path of the radiation in the material of about 0.1  $\mu\text{m}$ . At temperatures between 3000 and 4000 K, the maximum of the radiation spectrum in  $\text{UO}_2$  lies in the wavelength range 400-1000 nm as shown in Fig. 10. Because of the high opacity of liquid  $\text{UO}_2$  in this spectral range, the radiative heat transfer cannot contribute significantly to the thermal conductivity.

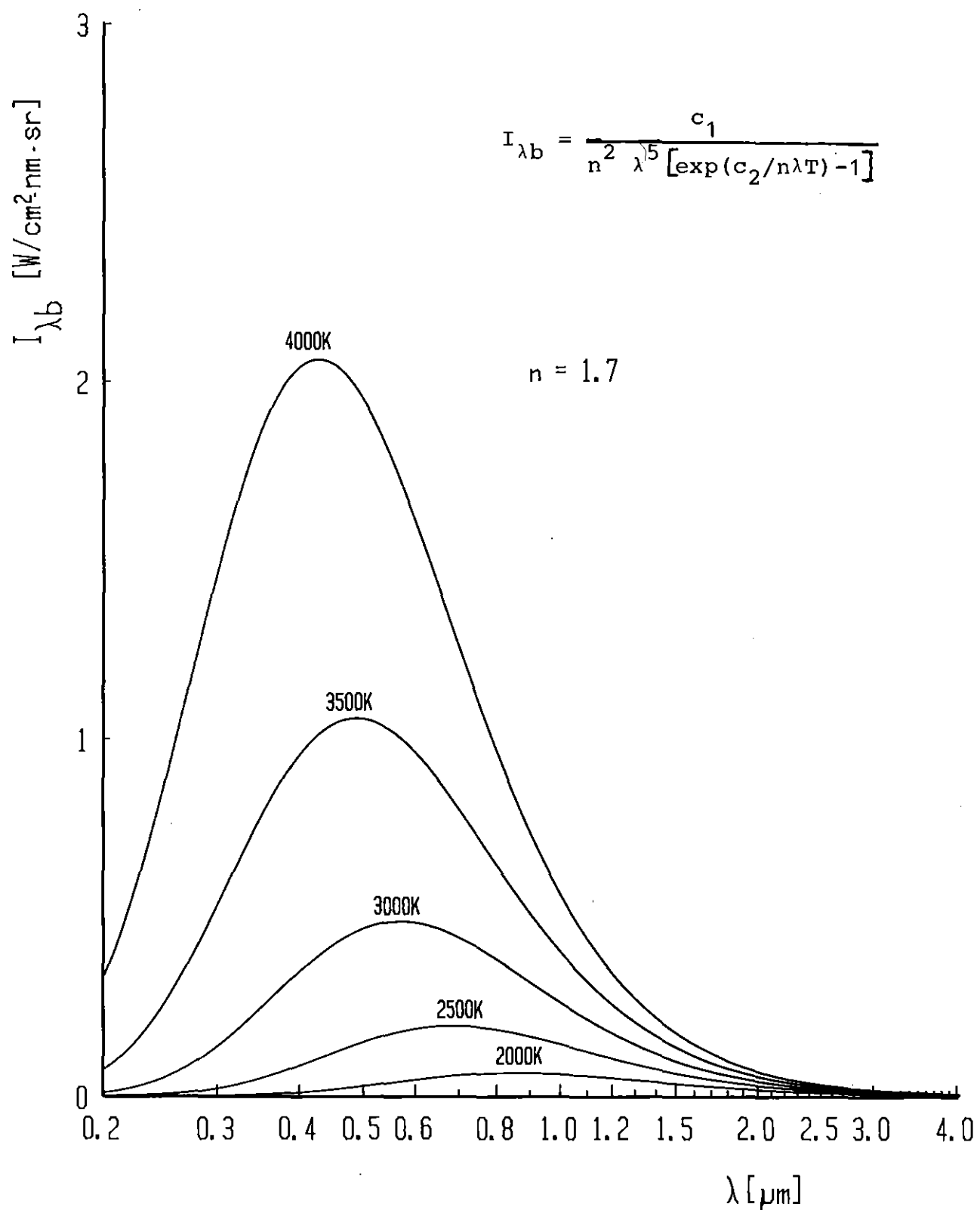


Fig.10: Planck black body radiation within a medium with  $n=1.7$ .

References

1. C.S. Kim, R.A. Blomquist, J. Haley, R. Land, J. Fischer, M.G. Chasanov, L. Leibowitz:  
"Measurement of Thermal Diffusivity of Molten UO<sub>2</sub>", in Proceedings of the Seventh Symposium on Thermophysical Properties, Ed.A. Cezairliyan (New York: American Society of Mechanical Engineers), (1977), pp. 338-343.
2. E.E. Anderson:  
"Radiative Heat Transfer in Molten UO<sub>2</sub> Based on the Rosseland Diffusion Method", Nuclear Technology 30 (1976) 65-70.
3. R.A. Young:  
"Model for the Electronic Contribution to the Thermal and Transport Properties of ThO<sub>2</sub>, UO<sub>2</sub>, and PuO<sub>2</sub> in the Solid and Liquid Phases", J. Nucl. Mater. 87 (1979) 283-296.
4. D.A. MacInnes:  
"Do Electronic Transitions Contribute to the Thermodynamics of Condensed UO<sub>2</sub>? ", in Proceedings of the Symposium on Thermodynamics of Nuclear Materials 1979, Vienna: IAEA (1980) pp. 129-139.
5. P. Browning:  
"On the Relative Importance of the Electronic and Radiative Contributions to the Thermal Conductivity of Uranium Dioxide", J. Nucl. Mater. 92 (1980) 33-38.
6. R.J. Ackermann, R.J. Thorn, G.H. Winslow:  
"Visible and Ultraviolet Absorption Properties of Uranium Dioxide Films", J. Opt. Soc. Am- 49 (1959) 1107-1112.

7. J.L. Bates:

"Visible and Infrared Absorption Spectra of Uranium Dioxide", Nucl. Sci. Eng. 21 (1965) 26-29.

8. M.J. Davies:

"A Spectrometric Study of the Dioxides of Cerium, Thorium and Uranium", PH.D. Thesis, University of Leeds, Leeds, England, 1970.

9. M. Bober:

"Spectral Reflectivity and Emissivity of Solid and Liquid  $UO_2$  as a Function of Wavelength, Angle of Incidence, and Polarization", in Proceedings of the Seventh European Thermophysical Properties Conference, Antwerpen (Belgium) June 30 - July 4, 1980; High Temperatures - High Pressures 12 (1980) 297-306.

10. M. Bober, J. Singer, K. Wagner:

"Spectral Reflectivity and Emissivity Measurements of Solid and Liquid  $UO_2$  at 458, 514.5 and 647 nm as a Function of Polarization and Angle of Incidence", Report KfK 3023, Kernforschungszentrum Karlsruhe, Federal Republic of Germany (1980).

11. M. Bober, H.U. Karow:

"Measurements of Spectral Emissivity of  $UO_2$  above the Melting Point", in Proceedings of the Seventh Symposium on Thermophysical Properties, Ed. A. Cezairliyan (New York: American Society of Mechanical Engineers), (1977) pp. 334-350.

12. K. Müller:

"Messung des spektralen Emissionsvermögens von keramischen Materialien im festen und im flüssigen Zustand mit einem Laser-Reflektometer", Report KfK 2803, Kernforschungszentrum Karlsruhe, Federal Republic of Germany (1979).

13. F. Grum, M. Saltzman:

"New White Standard of Reflectance", P-75-77, Comptes Rendus 18<sup>e</sup> Session,  
Londres 1975, CIE Publication Paris No. 36.1966, pp.91-97.

14. M. Bober, H.U. Karow, K. Miller:

"Study of the Spectral Reflectivity and Emissivity of Liquid Ceramics",  
High Temperatures - High Pressures 12 (1980) 161-168 .

15. M.N. Özisik:

"Radiative Transfer", Wiley, New York, 1973.

16. E.N. Shestakov, L.N. Latyev, V. Ya.Chekhovskoi:

"Methods for Determining the Optical Constants of Metals and Alloys at High  
Temperatures (Survey)", High Temperatures 16, 140 (1978) 140-151 (Translated  
from Russian, Teplofizika Vysokikh Temperatur 16 (1978) 178-189).

17. D.G. Avery:

"An Improved Method for Measurements of Optical Constants by Reflection",  
Proc. Phys. Soc. B65 (1952) 425-428.

18. M. Born, E. Wolf:

"Principles of Optics", Pergamon Press, Oxford, 1975 .

19. H.B. Holl:

"Numerical Solutions of the Fresnel Equations in the Optical Region",  
in Proceedings of the Symposium on Thermal Radiation of Solids, Ed. S. Katzoff  
(Washington DC, USA: National Aeronautics and Space Administration) Report  
NASA SP-55 (1965) pp. 45-61.

20. W.R. Hunter:

"Errors in Using the Reflectance vs. Angle of Incidence Method for Measuring Optical Constants", J. Opt. Soc. Am. 55, (1965) 1197-1204.

**Table IV** Measured reflectivities of liquid  $\text{UO}_2$  for the parallel ( $\rho_{\parallel}$ ) and the perpendicular ( $\rho_{\perp}$ ) components at the wavelengths 458, 514.5, 647.1 and 752.5 nm and the angles of incidence  $45^\circ$ ,  $58^\circ$  and  $71^\circ$

$\lambda = 458.0 \text{ nm}$ ,  $\theta = 45^\circ$

T [K]	$\rho_{\parallel}$	T [K]	$\rho_{\parallel}$	T [K]	$\rho_{\perp}$	T [K]	$\rho_{\perp}$
3787	0.034	3512	0.074	3792	0.154	3579	0.206
3784	0.055	3495	0.050	3772	0.161	3549	0.228
3738	0.034	3398	0.078	3763	0.191	3529	0.254
3718	0.047	3304	0.063	3734	0.184	3517	0.253
3705	0.051	3255	0.083	3729	0.173	3475	0.247
3667	0.058	3209	0.092	3720	0.206	3471	0.246
3650	0.050	3196	0.069	3719	0.163	3423	0.273
3630	0.054	3195	0.069	3688	0.187	3423	0.274
3626	0.064	3182	0.085	3685	0.181	3399	0.264
3622	0.042	3168	0.083	3676	0.211	3248	0.278
3608	0.065	3117	0.068	3666	0.194	3189	0.298
3593	0.047	3117	0.089	3662	0.211	3118	0.301
3588	0.057	3102	0.079	3625	0.212	3118	0.288
3582	0.069	3099	0.101	3620	0.204	3116	0.285
3579	0.050	3097	0.092	3598	0.207	3116	0.267
3539	0.053	3093	0.073	3584	0.249	3108	0.261
3517	0.063	3037	0.095	3581	0.232	3106	0.253
				3580	0.210	3105	0.307
				3580	0.240	3103	0.263

$\lambda = 458.0 \text{ nm}$ ,  $\theta = 58^\circ$

T [K]	$\rho_{\parallel}$	T [K]	$\rho_{\parallel}$	T [K]	$\rho_{\perp}$	T [K]	$\rho_{\perp}$
3723	0.033	3422	0.034	3729	0.245	3531	0.306
3717	0.021	3393	0.035	3723	0.235	3529	0.328
3709	0.023	3393	0.035	3707	0.241	3527	0.261
3680	0.020	3336	0.038	3704	0.224	3497	0.307
3668	0.036	3320	0.047	3696	0.231	3481	0.301
3657	0.025	3319	0.031	3694	0.247	3445	0.313
3656	0.024	3288	0.042	3694	0.241	3433	0.319
3596	0.031	3244	0.047	3676	0.241	3423	0.327
3590	0.029	3219	0.040	3656	0.293	3417	0.292
3590	0.027	3199	0.041	3650	0.262	3385	0.340
3589	0.037	3199	0.041	3647	0.254	3335	0.349
3589	0.027	3184	0.050	3642	0.234	3331	0.341
3581	0.021	3174	0.044	3593	0.301	3275	0.363
3579	0.027	3165	0.036	3591	0.316	3262	0.311
3579	0.028	3157	0.048	3587	0.303	3219	0.375
3557	0.042	3140	0.039	3574	0.279	3143	0.345
3554	0.031	3137	0.043	3564	0.270	3139	0.366
3548	0.034	3127	0.049	3560	0.273	3137	0.344
3547	0.033	3126	0.033	3559	0.284	3136	0.344
3546	0.029	3126	0.042	3552	0.291	3124	0.339
3525	0.032	3126	0.038	3538	0.281	3120	0.372
3520	0.034	3126	0.049	3533	0.334	3119	0.346
3512	0.031	3122	0.047	3533	0.313	3093	0.376
3511	0.033	3121	0.040				
3498	0.032	3117	0.046				
3494	0.033	3116	0.046				
3490	0.038	3113	0.053				
3489	0.029	3112	0.053				
3466	0.030	3110	0.040				
3430	0.031	3101	0.037				
3427	0.031	3074	0.051				

$\lambda = 458.0 \text{ nm}$ ,  $\theta = 71^\circ$

T [K]	$\rho_{\parallel}$	T [K]	$\rho_{\parallel}$	T [K]	$\rho_{\perp}$	T [K]	$\rho_{\perp}$
3887	0.037	3720	0.053	3861	0.187	3461	0.426
3882	0.037	3710	0.053	3841	0.184	3430	0.438
3880	0.029	3691	0.046	3825	0.200	3299	0.471
3877	0.029	3658	0.048	3798	0.197	3269	0.454
3864	0.031	3574	0.047	3787	0.178	3259	0.466
3863	0.037	3477	0.047	3786	0.244	3174	0.494
3860	0.041	3401	0.048	3701	0.350	3136	0.502
3853	0.035	3398	0.050	3690	0.300	3107	0.536
3845	0.044	3390	0.051	3669	0.268	3105	0.549
3841	0.037	3376	0.060	3638	0.330	3104	0.540
3804	0.043	3271	0.068	3607	0.377	3103	0.527
3803	0.042	3259	0.061	3576	0.370	3072	0.544
3802	0.037	3259	0.061	3521	0.366	3048	0.510
3795	0.049	3204	0.057	3495	0.411	3035	0.566
3769	0.039	3127	0.087				
3757	0.053	3108	0.079				
3757	0.037	3103	0.083				
3753	0.053	3101	0.067				
3751	0.038	3098	0.077				
3745	0.044	3098	0.072				
3745	0.056	3095	0.072				
3741	0.033	3086	0.061				
3728	0.042	3060	0.059				

$\lambda = 514.5 \text{ nm}$ ,  $\theta = 45^\circ$

T [K]	$\rho_{\parallel}$	T [K]	$\rho_{\parallel}$	T [K]	$\rho_{\perp}$	T [K]	$\rho_{\perp}$
3675	0.035	3481	0.034	3861	0.103	3455	0.237
3631	0.043	3466	0.056	3843	0.075	3446	0.267
3616	0.050	3446	0.062	3799	0.101	3386	0.246
3611	0.040	3356	0.086	3784	0.115	3371	0.260
3606	0.042	3346	0.044	3775	0.116	3370	0.253
3602	0.035	3322	0.060	3761	0.127	3359	0.271
3584	0.041	3265	0.057	3745	0.118	3309	0.239
3559	0.038	3239	0.078	3728	0.158	3294	0.238
3559	0.038	3223	0.059	3670	0.146	3280	0.269
3557	0.041	3218	0.061	3641	0.184	3277	0.239
3554	0.054	3172	0.101	3628	0.180	3268	0.273
3553	0.055	3109	0.065	3593	0.220	3250	0.256
3542	0.055	3106	0.072	3591	0.197	3233	0.276
3536	0.053	3098	0.072	3564	0.234	3222	0.285
3531	0.056	3097	0.069	3552	0.185	3219	0.275
3529	0.035	3093	0.081	3532	0.195	3190	0.255
3526	0.057	3091	0.065	3522	0.248	3126	0.284
3525	0.036	3091	0.070	3514	0.251	3118	0.296
3523	0.049	3079	0.096	3495	0.207	3117	0.284
3511	0.043	3079	0.105	3492	0.214	3105	0.266
3488	0.072	3053	0.097	3479	0.250	3104	0.240
				3474	0.230	3102	0.271
				3473	0.254	3087	0.257
				3470	0.254	3086	0.258
				3468	0.247	3080	0.292
				3465	0.195	3080	0.284

$\lambda = 514.5 \text{ nm}, \theta = 58^\circ$ 

T [K]	$\rho_{\parallel}$	T [K]	$\rho_{\parallel}$	T [K]	$\rho_{\perp}$	T [K]	$\rho_{\perp}$
3701	0.016	3487	0.022	3883	0.128	3502	0.295
3639	0.016	3452	0.030	3878	0.129	3499	0.250
3636	0.020	3388	0.031	3843	0.142	3470	0.291
3593	0.018	3333	0.031	3751	0.163	3439	0.308
3586	0.021	3296	0.030	3740	0.174	3386	0.273
3583	0.020	3218	0.034	3673	0.209	3352	0.336
3579	0.020	3177	0.032	3627	0.240	3315	0.309
3573	0.025	3139	0.035	3626	0.242	3305	0.338
3570	0.023	3107	0.034	3618	0.233	3235	0.323
3568	0.019	3106	0.030	3615	0.216	3121	0.370
3565	0.022	3105	0.027	3603	0.272	3114	0.342
3547	0.022	3103	0.037	3585	0.231	3092	0.340
3546	0.026	3102	0.028	3579	0.271	3086	0.339
3545	0.025	3102	0.027	3552	0.266	3084	0.371
3541	0.026	3070	0.040	3544	0.258	3074	0.356
3541	0.024			3517	0.303	3071	0.347

 $\lambda = 514.5 \text{ nm}, \theta = 71^\circ$ 

T [K]	$\rho_{\parallel}$	T [K]	$\rho_{\parallel}$	T [K]	$\rho_{\perp}$	T [K]	$\rho_{\perp}$
3836	0.030	3358	0.078	3773	0.217	3354	0.410
3732	0.046	3335	0.065	3750	0.242	3301	0.405
3728	0.031	3330	0.045	3728	0.268	3270	0.470
3672	0.031	3312	0.062	3698	0.321	3228	0.483
3667	0.047	3301	0.071	3687	0.297	3179	0.447
3662	0.038	3288	0.059	3676	0.270	3123	0.508
3654	0.050	3282	0.066	3650	0.288	3121	0.492
3632	0.044	3266	0.068	3635	0.278	3103	0.510
3629	0.042	3240	0.063	3614	0.330	3099	0.504
3624	0.039	3207	0.066	3592	0.367	3098	0.517
3605	0.047	3171	0.071	3588	0.296	3077	0.474
3594	0.042	3133	0.056	3572	0.377	3073	0.516
3592	0.036	3119	0.063	3564	0.351	3072	0.511
3585	0.057	3116	0.067	3528	0.309	3072	0.513
3557	0.055	3116	0.068	3509	0.309	3071	0.488
3548	0.050	3110	0.076	3430	0.345	3062	0.519
3546	0.046	3109	0.043	3409	0.391	3030	0.535
3545	0.043	3109	0.069	3380	0.441		
3524	0.047	3107	0.049				
3519	0.055	3103	0.063				
3515	0.055	3101	0.043				
3514	0.054	3101	0.072				
3499	0.055	3095	0.069				
3498	0.060	3095	0.083				
3480	0.050	3095	0.075				
3452	0.058	3092	0.067				
3429	0.069	3086	0.067				
3419	0.060	3086	0.053				
3414	0.051	3070	0.063				
3402	0.062						

$\lambda = 647.1 \text{ nm}$ ,  $\theta = 45^\circ$ 

T [K]	$\rho_{\parallel}$	T [K]	$\rho_{\parallel}$	T [K]	$\rho_{\perp}$	T [K]	$\rho_{\perp}$
3822	0.046	3479	0.059	3874	0.124	3624	0.215
3822	0.046	3467	0.061	3855	0.127	3617	0.207
3813	0.036	3466	0.055	3841	0.144	3613	0.206
3786	0.046	3460	0.062	3841	0.107	3587	0.230
3763	0.048	3428	0.061	3839	0.126	3544	0.238
3757	0.038	3410	0.051	3811	0.136	3538	0.221
3744	0.049	3400	0.056	3796	0.145	3522	0.233
3740	0.047	3370	0.052	3792	0.145	3429	0.239
3725	0.032	3313	0.065	3788	0.151	3390	0.259
3710	0.048	3310	0.058	3786	0.156	3376	0.229
3706	0.046	3293	0.067	3775	0.150	3321	0.238
3694	0.058	3246	0.055	3758	0.143	3316	0.236
3678	0.042	3246	0.068	3758	0.169	3313	0.255
3672	0.054	3238	0.072	3734	0.167	3250	0.246
3670	0.046	3230	0.070	3729	0.170	3233	0.265
3663	0.040	3196	0.074	3726	0.175	3162	0.252
3656	0.047	3155	0.064	3721	0.173	3135	0.256
3633	0.050	3154	0.074	3721	0.185	3116	0.254
3621	0.046	3130	0.080	3718	0.190	3115	0.250
3619	0.052	3128	0.078	3706	0.164	3114	0.253
3605	0.052	3117	0.071	3706	0.194	3106	0.232
3589	0.067	3116	0.065	3697	0.174	3106	0.260
3574	0.053	3112	0.062	3696	0.192	3106	0.238
3565	0.046	3110	0.082	3686	0.191	3101	0.251
3543	0.049	3107	0.067	3675	0.200	3098	0.278
3539	0.059	3106	0.073	3670	0.199	3097	0.274
3536	0.057	3103	0.074	3664	0.193	3096	0.263
3530	0.056	3089	0.081	3657	0.192	3089	0.239
3502	0.061	3089	0.070	3652	0.194	3082	0.245
3491	0.057	3079	0.073				

 $\lambda = 647.1 \text{ nm}$ ,  $\theta = 58^\circ$ 

T [K]	$\rho_{\parallel}$	T [K]	$\rho_{\parallel}$	T [K]	$\rho_{\perp}$	T [K]	$\rho_{\perp}$
3693	0.026	3422	0.033	3698	0.240	3525	0.289
3679	0.019	3416	0.028	3691	0.242	3524	0.287
3669	0.031	3395	0.030	3683	0.246	3510	0.310
3655	0.027	3383	0.026	3664	0.253	3504	0.320
3633	0.032	3358	0.033	3657	0.242	3495	0.296
3630	0.025	3323	0.026	3656	0.254	3495	0.307
3622	0.025	3310	0.034	3653	0.278	3490	0.316
3617	0.027	3271	0.029	3633	0.263	3482	0.301
3611	0.031	3245	0.034	3627	0.257	3455	0.307
3593	0.030	3192	0.034	3626	0.256	3417	0.328
3571	0.026	3132	0.028	3626	0.262	3415	0.325
3560	0.031	3129	0.028	3623	0.263	3404	0.316
3558	0.023	3126	0.036	3619	0.260	3390	0.320
3552	0.025	3120	0.036	3618	0.266	3379	0.321
3552	0.025	3118	0.037	3612	0.273	3366	0.313
3549	0.029	3111	0.036	3612	0.291	3352	0.329
3523	0.026	3110	0.036	3602	0.285	3297	0.330
3476	0.033	3105	0.038	3598	0.291	3283	0.326
3467	0.032	3095	0.034	3587	0.253	3283	0.333
				3585	0.266	3238	0.354
				3584	0.288	3230	0.339
				3579	0.285	3224	0.356
				3575	0.269	3138	0.349
				3574	0.269	3137	0.337
				3570	0.293	3128	0.369
				3547	0.291	3126	0.353
				3533	0.303	3122	0.372

$\lambda = 647.1 \text{ nm}$ , $\theta = 71^\circ$ 

- 28 -

T [K]	$\rho_{\parallel}$	T [K]	$\rho_{\parallel}$	T [K]	$\rho_{\perp}$	T [K]	$\rho_{\perp}$
3877	0.032	3681	0.038	3875	0.202	3695	0.316
3870	0.038	3659	0.040	3872	0.254	3620	0.350
3870	0.032	3645	0.048	3872	0.221	3602	0.380
3866	0.029	3637	0.040	3855	0.191	3558	0.353
3865	0.027	3619	0.040	3854	0.248	3502	0.397
3860	0.030	3615	0.038	3850	0.234	3465	0.361
3860	0.033	3577	0.039	3846	0.251	3453	0.411
3854	0.034	3571	0.044	3843	0.242	3446	0.421
3849	0.030	3533	0.042	3835	0.226	3434	0.431
3844	0.033	3522	0.046	3832	0.225	3429	0.427
3843	0.034	3487	0.040	3830	0.235	3424	0.372
3839	0.036	3482	0.044	3830	0.270	3368	0.427
3832	0.038	3466	0.049	3819	0.224	3343	0.462
3821	0.033	3432	0.048	3818	0.249	3249	0.456
3819	0.037	3416	0.047	3817	0.231	3176	0.477
3813	0.035	3415	0.049	3810	0.245	3163	0.458
3798	0.039	3412	0.046	3809	0.244	3138	0.476
3798	0.033	3378	0.048	3801	0.291	3108	0.489
3794	0.041	3361	0.057	3800	0.264	3101	0.500
3792	0.041	3338	0.048	3785	0.278	3096	0.521
3787	0.035	3323	0.054	3782	0.289	3086	0.458
3786	0.042	3297	0.051	3755	0.269	3079	0.449
3762	0.040	3257	0.054	3751	0.320	3069	0.457
3761	0.037	3247	0.056	3717	0.356	3069	0.486
3747	0.035	3198	0.054	3697	0.274	3068	0.454
3736	0.046	3115	0.066				
3736	0.034	3112	0.055				
3731	0.039	3108	0.068				
3726	0.046	3097	0.056				
3685	0.041	3093	0.066				
3682	0.048	3067	0.062				

 $\lambda = 752.5 \text{ nm}$ , $\theta = 45^\circ$ 

T [K]	$\rho_{\parallel}$	T [K]	$\rho_{\parallel}$	T [K]	$\rho_{\perp}$	T [K]	$\rho_{\perp}$
3794	0.042	3448	0.051	3866	0.164	3632	0.243
3778	0.038	3437	0.070	3861	0.169	3606	0.233
3764	0.039	3399	0.068	3856	0.171	3585	0.252
3755	0.036	3357	0.078	3850	0.175	3574	0.229
3736	0.045	3329	0.071	3849	0.155	3507	0.254
3730	0.037	3302	0.074	3840	0.170	3507	0.251
3699	0.060	3291	0.084	3831	0.165	3503	0.263
3683	0.047	3287	0.075	3825	0.192	3499	0.254
3659	0.054	3231	0.081	3814	0.159	3482	0.231
3650	0.044	3172	0.092	3803	0.181	3459	0.258
3646	0.052	3143	0.093	3798	0.211	3433	0.272
3639	0.054	3133	0.084	3790	0.178	3387	0.249
3635	0.058	3117	0.083	3785	0.166	3362	0.278
3619	0.046	3116	0.075	3778	0.206	3320	0.269
3618	0.064	3110	0.081	3773	0.165	3320	0.289
3596	0.051	3105	0.088	3758	0.216	3194	0.279
3568	0.047	3102	0.070	3756	0.200	3128	0.293
3567	0.048	3101	0.092	3748	0.185	3115	0.307
3555	0.056	3087	0.093	3739	0.182	3110	0.279
3552	0.056	3087	0.081	3700	0.209	3104	0.288
3525	0.056	3081	0.093	3682	0.194	3103	0.294
3500	0.058	3080	0.079	3681	0.209	3096	0.281
3462	0.065	3076	0.092	3672	0.221	3092	0.263
3460	0.064			3668	0.203	3083	0.287
				3664	0.210	3081	0.291
				3654	0.212	3078	0.293
				3652	0.239	3068	0.291

$\lambda = 752.5 \text{ nm}, \theta = 58^\circ$ 

T [K]	$\rho_{\parallel}$	T [K]	$\rho_{\parallel}$	T [K]	$\rho_{\perp}$	T [K]	$\rho_{\perp}$
3747	0.027	3447	0.035	3793	0.224	3456	0.331
3733	0.031	3423	0.042	3736	0.266	3450	0.332
3727	0.028	3407	0.044	3728	0.293	3417	0.333
3710	0.034	3380	0.050	3721	0.218	3370	0.348
3695	0.035	3358	0.053	3715	0.237	3277	0.349
3693	0.035	3352	0.047	3699	0.237	3213	0.380
3689	0.037	3249	0.040	3696	0.289	3191	0.386
3672	0.034	3142	0.041	3690	0.259	3170	0.390
3671	0.029	3131	0.042	3658	0.254	3124	0.420
3671	0.026	3127	0.043	3656	0.249	3122	0.364
3659	0.036	3122	0.052	3654	0.289	3121	0.359
3656	0.043	3112	0.038	3641	0.314	3114	0.379
3655	0.039	3110	0.062	3636	0.288	3111	0.371
3651	0.036	3103	0.045	3602	0.251	3107	0.403
3651	0.036	3103	0.045	3595	0.278	3103	0.398
3648	0.040	3098	0.041	3582	0.310	3093	0.367
3600	0.028	3097	0.045	3578	0.300	3091	0.396
3581	0.028	3095	0.050	3483	0.291	3078	0.426
3577	0.032	3095	0.047	3465	0.373	3066	0.362
3572	0.036	3094	0.044				
3556	0.033	3094	0.042				
3533	0.042	3091	0.061				
3509	0.043	3085	0.055				
3504	0.042	3082	0.052				
3463	0.039	3081	0.060				
3454	0.036	3063	0.065				

 $\lambda = 752.5 \text{ nm}, \theta = 71^\circ$ 

T [K]	$\rho_{\parallel}$	T [K]	$\rho_{\parallel}$	T [K]	$\rho_{\perp}$	T [K]	$\rho_{\perp}$
3764	0.036	3472	0.047	3812	0.279	3585	0.412
3762	0.039	3460	0.071	3801	0.289	3569	0.423
3760	0.046	3458	0.064	3781	0.295	3551	0.361
3748	0.055	3397	0.061	3770	0.283	3542	0.372
3746	0.054	3341	0.057	3767	0.327	3536	0.403
3745	0.040	3331	0.065	3766	0.275	3499	0.360
3742	0.039	3305	0.074	3763	0.315	3451	0.388
3721	0.046	3299	0.071	3762	0.293	3421	0.424
3721	0.045	3261	0.069	3762	0.293	3412	0.394
3718	0.036	3227	0.072	3757	0.328	3399	0.387
3705	0.037	3212	0.078	3751	0.362	3387	0.453
3692	0.053	3207	0.087	3735	0.353	3342	0.436
3691	0.041	3130	0.063	3734	0.301	3336	0.408
3683	0.053	3128	0.069	3715	0.366	3304	0.474
3679	0.058	3126	0.075	3704	0.319	3268	0.476
3657	0.044	3106	0.065	3703	0.356	3233	0.452
3654	0.057	3104	0.070	3701	0.352	3172	0.500
3638	0.057	3102	0.058	3694	0.315	3169	0.486
3635	0.052	3096	0.083	3674	0.383	3167	0.469
3634	0.057	3068	0.061	3656	0.318	3148	0.518
3612	0.062	3065	0.081	3655	0.358	3134	0.490
3583	0.054	3055	0.080	3639	0.364	3102	0.510
3565	0.043	3055	0.080	3638	0.368	3101	0.507
3550	0.062			3637	0.325	3100	0.537
				3609	0.342	3092	0.525
				3600	0.324	3071	0.495